Cell, Vol. 121, 281–293, April 22, 2005, Copyright ©2005 by Elsevier Inc. DOI 10.1016/j.cell.2005.02.036

The Strength of Receptor Signaling Is Centrally Controlled through a Cooperative Loop between Ca^{2+} and an Oxidant Signal

Dinesh Kumar Singh, Dhiraj Kumar, Zaved Siddiqui, Sandip Kumar Basu, Vikas Kumar, and Kanury V.S. Rao*
Immunology Group
International Centre for Genetic Engineering and Biotechnology
Aruna Asaf Ali Marg
New Delhi 110067
India

Summary

Activation of cell-surface receptors stimulates generation of intracellular signals that, in turn, direct the cellular response. However, mechanisms that ensure combinatorial control of these signaling events are not well understood. We show here that the Ca^{2+} and reactive oxygen intermediates generated upon BCR activation rapidly engage in a cooperative interaction that acts in a feedback manner to amplify the early signal generated. This cooperativity acts by regulating the concentration of the oxidant produced. The latter exerts its influence through a pulsed inactivation of receptor-coupled phosphatases, where the amplitude of this pulse is determined by oxidant concentration. The extent of phosphatase inhibition, in turn, dictates what proportion of receptor-proximal kinases are activated and, as a result, the net strength of the initial signal. It is the strength of this initial signal that finally determines the eventual duration of BCR signaling and the rate of its transmission through downstream pathways.

Introduction

Binding of a ligand to a cell-surface receptor often stimulates an elaborate cascade of signal-transduction events. Rather than simply represent a linear transmission of information, proteins involved in signaling build complex intracellular networks in which signal propagation is controlled in a combinatorial manner (Pawson and Saxton, 1999; Weng et al., 1999). In addition to transmission, information processing also represents a key aspect of intracellular signaling. The functioning of feedback loops that regulate—either positively or negatively—perpetuation of individual modular constituents of the signaling pathways largely facilitates such processing (Bhalla and Iyengar, 1999; Ferrell, 2002). In addition, by regulating formation of multimolecular assemblies, scaffold (or adaptor) proteins have also been implicated in the regulation of signal transduction (Pawson and Scott, 1997; Smith and Scott, 2002). While the complexity of signaling pathways is being increasingly appreciated, details about how signal output is modulated are yet to be elucidated. Some of the parameters that constitute variables in the output are the amplitude and duration of signal, in addition to the rate at which it is transmitted. Little is known, however, about how context-dependent regulation of these parameters is achieved (Heinrich et al., 2002).

Lymphocytes provide good model systems for the study of signal plasticity. Variations in the nature of antigen-receptor-dependent signaling are known to produce a variety of outcomes ranging from cell proliferation and differentiation on the one hand to cell death on the other. The B lymphocyte antigen receptor (BCR) is a hetero-oligomeric transmembrane protein in which the surface immunoglobulin (sIg) constitutes the ligand binding unit, whereas the signaling function is encoded within the noncovalently associated heterodimer of CD79a and CD79b (Schamel and Reth, 2000). Three distinct families of cytoplasmic protein tyrosine kinases (PTKs)—Src, Syk, and Btk—mediate BCR activation, with activation of the Src PTKs serving as the critical first step. The activated BCR then recruits several downstream signaling pathways, some of which are those dependent upon PLCγ, the Rho family of GTPases, and the Ras/PI-3-K (Kurosaki, 2002).

In this study we examined the dynamics and possible regulatory mechanisms of signal propagation from the BCR. We provide evidence to suggest that it is the strength of the initial signal generated that controls both the rate and extent of its subsequent progression through the downstream pathways. The former, in turn, is shown to depend upon a positive feedback loop that was rapidly established between two BCR-dependent second messengers, Ca_i^{2+} and reactive oxygen species (ROS). A rheostat-like function could be assigned to this loop, in terms of regulating the amplitude and duration of BCR signaling.

Results

Calcium Dependency of BCR Signaling

We monitored intracellular phosphorylation events in A20 cells, a murine B cell lymphoma cell line that expresses surface immunoglobulin receptors of the IgG2a isotype. Cells were pre-equilibrated with [^{32}P]-orthophosphoric acid prior to stimulation with the $F(ab)_2$ fragment of anti-mouse IgG (anti-IgG), and the lysates were subsequently resolved by two-dimensional gel electrophoresis (2-DE) for analysis by autoradiography. Ligation of the BCR also leads to the mobilization of free calcium ions in the cytoplasm (Ca_i^{2+}), which constitute important intracellular second messengers for BCR signaling. Therefore, we also examined for the consequences of either complete or partial blockage of the Ca_i^{2+} response. BCR-dependent Ca_i^{2+} recruitment occurs in two distinct phases, the first of which involves its release from the intracellular stores in the endoplasmic reticulum (ER). Exhaustion of these stores activates calcium-release-activated channels, which then promote influx of Ca^{2+} from the extracellular medium (Winslow et al., 2003). This latter phase is known as capacitative calcium entry (CCE). The pharmacologi-

*Correspondence: kanury@icgeb.res.in

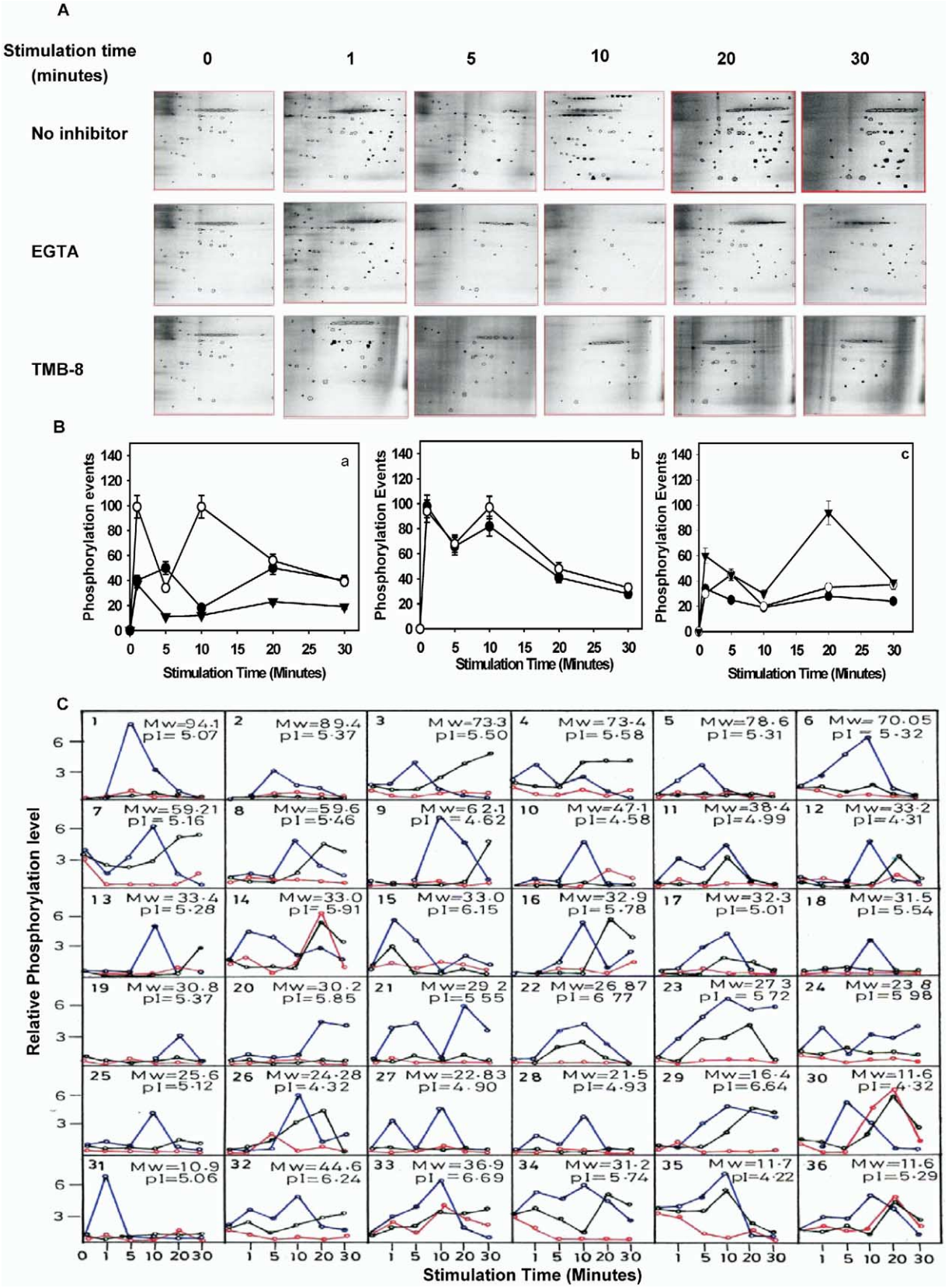
A
Stimulation time (minutes)
0
1
5
10
20
30
No inhibitor
EGTA
TMB-8
B
a
b
c
Phosphorylation events
Phosphorylation Events
Stimulation Time (Minutes)
C
Relative Phosphorylation level
1 Mw=94.1 pI=5.07
2 Mw=89.4 pI=5.37
3 Mw=73.3 pI=5.50
4 Mw=73.4 pI=5.58
5 Mw=78.6 pI=5.31
6 Mw=70.05 pI=5.32
7 Mw=59.21 pI=5.16
8 Mw=59.6 pI=5.46
9 Mw=62.1 pI=4.62
10 Mw=47.1 pI=4.58
11 Mw=38.4 pI=4.99
12 Mw=33.2 pI=4.31
13 Mw=33.4 pI=5.28
14 Mw=33.0 pI=5.91
15 Mw=33.0 pI=6.15
16 Mw=32.9 pI=5.78
17 Mw=32.3 pI=5.01
18 Mw=31.5 pI=5.54
19 Mw=30.8 pI=5.37
20 Mw=30.2 pI=5.85
21 Mw=29.2 pI=5.55
22 Mw=26.87 pI=6.77
23 Mw=27.3 pI=5.72
24 Mw=23.8 pI=5.98
25 Mw=25.6 pI=5.12
26 Mw=24.28 pI=4.32
27 Mw=22.83 pI=4.90
28 Mw=21.5 pI=4.93
29 Mw=16.4 pI=6.64
30 Mw=11.6 pI=4.32
31 Mw=10.9 pI=5.06
32 Mw=44.6 pI=6.24
33 Mw=36.9 pI=6.69
34 Mw=31.2 pI=5.74
35 Mw=11.7 pI=4.22
36 Mw=11.6 pI=5.29
Stimulation Time (Minutes)

cal agent TMB-8 inhibits calcium release from the ER, thereby completely inhibiting the BCR-dependent Ca_i^{2+} response (Kubohara and Hosaka, 1999). In contrast, EGTA can be used to selectively block CCE through chelation of extracellular Ca^{2+} (Dolmetsch et al., 1998) (Figure S1).

The results obtained from such experiments are shown in Figure 1A. Stimulation of cells with anti-IgG led to an increase in the number of phosphoproteins that were detectable. However, inclusion of either EGTA or TMB-8 proved inhibitory to this response, with TMB-8 showing the more pronounced effect. Figure 1B presents an analysis of the number of phosphoproteins detected at each time point after ensuring that these were not present in the corresponding profile for unstimulated cells. Two "waves" of phosphorylation were evident in cells stimulated in the absence of a Ca_i^{2+} inhibitor (Figure 1Ba). The first, which peaked by 1 min of stimulation time and declined thereafter up to 5 min of stimulation, involved rapid phosphorylation of about 100 proteins. A resurgent phase of phosphorylation of 97 newly phosphorylated proteins was then detected to peak by 10 min of stimulation and was followed by a gradual decline in the number of phosphoproteins that persisted over the remainder of the experiment. A careful comparison of the autoradiograms obtained at 1 min and 10 min of stimulation revealed that only 21 of the radiolabeled proteins were common to both time points. Thus, the phosphorylation peak detected at 10 min predominantly occurs on new substrates that represent downstream components of BCR signaling. Some of the phosphoproteins from these two time points could also be identified by mass spectrometry (Figures S2 and S3).

Stimulation of cells in the presence of EGTA led to a dampening of BCR signal, where a marked reduction in intensity of both phosphorylation peaks was clearly evident (Figure 1Ba). In addition to the quantitative effect, a delay in the kinetics of phosphorylation was also discernable. The phosphoproteins observed in both the 1 min and 5 min time points of cells stimulated in the presence of EGTA were all present in the 1 min peak from cells stimulated in the absence of an inhibitor. The peak spread in the presence of EGTA, therefore, describes delayed phosphorylation of some of the early BCR-dependent substrates. This kinetic effect was more pronounced in the second phase of phosphorylation, normally observed at 10 min in cells stimulated without any inhibitor. A comparison of the autoradiograms revealed that all of the radiolabeled spots detected at 20 min in cells stimulated in the presence of EGTA were present in the 10 min peak obtained in the absence of an inhibitor. That is, the inclusion of EGTA resulted in a delay of 10 min in the phosphorylation of this subset of proteins. Finally, attenuation of BCR signaling was even more marked when cells were stimulated in the presence of TMB-8. Here the early phase was severely inhibited, with subsequent events being virtually undetectable (Figure 1Ba).

That our results describe Ca_i^{2+} dependency rather than nonspecific effects of the inhibitors was verified by the following additional experiments. The effects of both EGTA and TMB-8 could be completely reversed under conditions of calcium supplementation (Figure 1Bb). Furthermore, stimulation of cells in the presence of Ca^{2+}-deficient medium also yielded results similar to those obtained with EGTA, whereas substantial signal dampening was observed in cells stimulated in the presence of the cell-permeable chelator of intracellular Ca^{2+}, BAPTA-AM (Figure 1Bc). Finally, we also transfected A20 cells with the gene coding for EhCaBP, a high-affinity Ca^{2+} binding protein derived from *Entamoeba histolytica* (Yadava et al., 1997). These cells displayed a partial suppression of the BCR-dependent Ca_i^{2+} response (Figure S1). The phosphorylation profile obtained in anti-IgG-stimulated EhCaBP-expressing cells is shown in Figure 1Bc. A significant reduction in amplitude of the first phase of signaling is clearly evident, although it was less pronounced than that obtained with EGTA. Interestingly, while the intensity of downstream signaling was largely unaffected, there was a substantial delay in its accrual, with the second peak of phosphorylation appearing only at 20 min of stimulation (Figure 1Bc).

Thus, the data in Figure 1Ba identify a graded effect in which selective blockage of CCE produces a less severe inhibition than that obtained upon complete suppression of BCR-dependent Ca_i^{2+} mobilization. It is presumably due to the profound inhibition of the early phase of signaling in the presence of TMB-8 that downstream signals also do not accumulate. In comparison, the relatively less pronounced effect of EGTA led to a situation where, in addition to attenuation, there was a "slowing down" of the partial signaling capability that was retained. This was especially evident for the second phase of phosphorylation, normally seen at 10 min in the absence of an inhibitor. In other words, the intensity of the first phase of signaling appears to have a significant impact on that of the downstream events, in addition to the kinetics of subsequent signal transmission.

Figure 1. Inhibition of BCR-Dependent Ca_i^{2+} Recruitment Inhibits BCR Signaling

(A) shows the autoradiograms obtained upon 2-DE resolution of the proteins from cells stimulated with anti-IgG under the conditions and for the times indicated. For clarity, only autoradiograms from regions spanning a Mw range of 15 to 75 kDa and a pI range of 5 to 7 are shown. (Ba) shows the number of new phosphorylation events at various times after stimulation in the absence (○) or presence of either 3 mM EGTA (●) or 100 mM TMB-8 (▼). (Bb) shows the number of new phosphorylation events in anti-IgG-stimulated cells where either EGTA was supplemented with 1.3 molar equivalent of $CaCl_2$ (○) or TMB-8 addition was combined with 2 mM ionomycin (●). (Bc) shows the profile for cells either stimulated in Ca^{2+}-free medium (○) or treated with BAPTA-AM (●), or for cells overexpressing EhCaBP (▼). The mock-transfected cells yielded a profile similar to that of uninhibited nontransfected cells. Values given are the mean (±SD) of three separate experiments. (C) illustrates relative changes in phosphorylation levels of the individual protein spots seen in (A). Data for a randomly selected set of 36 spots that are commonly present in cells stimulated in the absence (blue line) or presence of either EGTA (green line) or TMB-8 (red line) are shown. An arbitrary scale is used that reflects the relative levels of phosphorylation (mean values, n = 4) of each spot at the various time points.

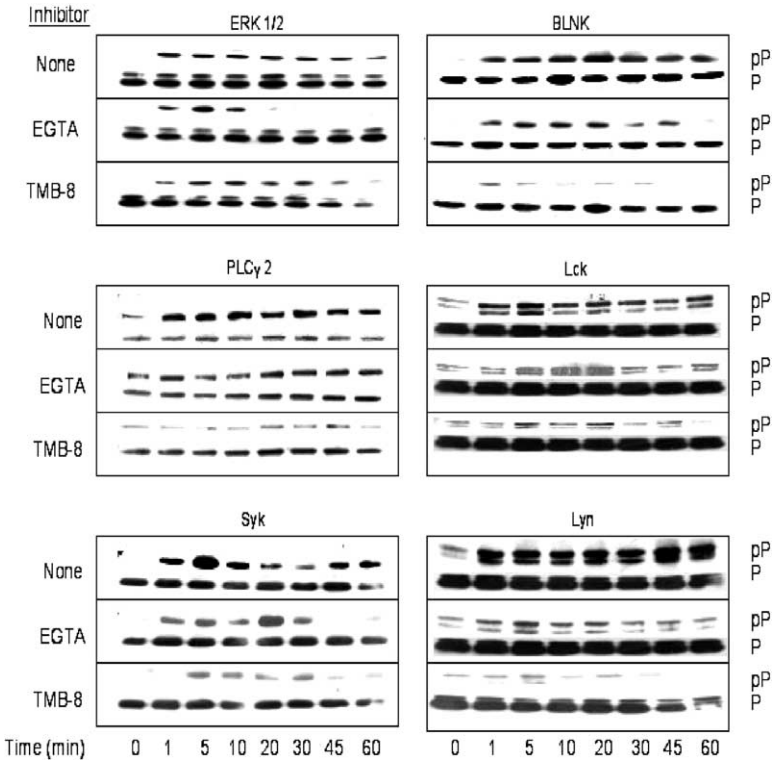

Figure 2. Ca_i^{2+} Dependency of BCR Substrate Phosphorylation

Cells were stimulated with anti-IgG for the indicated times in the absence (None) or presence of either EGTA or TMB-8. The phosphorylation status of the indicated proteins was then examined through immunoprecipitation with specific antibodies followed by Western blot for either the amount of target protein present (P) or the extent of its phosphorylation (pP). For the latter, anti-phosphotyrosine antibodies were used in all cases, except for ERK1/2, where anti-phospho-ERK antibodies were employed.

Figure 1C presents the kinetic profiles for individual randomly selected phosphoprotein spots. A significant effect of EGTA addition is clearly evident in virtually all of the cases examined and involved a reduction in either magnitude (e.g., spots 1, 2, 5, and 6), kinetics of phosphorylation (e.g., spots 3, 8, 16, 29, and 30), or both (e.g., spots 10, 12, and 25). As expected, TMB-8 addition produced a more complete inhibition relative to EGTA. The few exceptions nonetheless had to experience a significant time lag before undergoing phosphorylation. Thus, while the data in Figure 1B detail the time-dependent flux in phosphorylation events as a consequence of Ca_i^{2+} inhibition, the results in Figure 1C highlight that this flux was not restricted to a specific subset of target proteins. Rather, the latter describe it as a "global" phenomenon in which at least a significant proportion of intermediates in the BCR signaling pathway are affected.

The Regulatory Effect of Ca_i^{2+} Is Enforced through a Feedback Pathway

Next, we again performed the anti-IgG stimulation experiments, but in cells that were not labeled with radioactive phosphate. Lysates were immunoprecipitated with antibodies against known intermediates in BCR signaling, and the phosphorylation status of these targets was determined by Western blots. Regardless of the target probed, conditions of Ca_i^{2+} suppression consistently led to a decrease in the magnitude of phosphorylation, with TMB-8 showing the more pronounced effect relative to EGTA (Figure 2). A lag in maximal phosphorylation of Syk was also noted in the presence of EGTA. With the exception of ERK1/2, phosphorylation of all the remaining proteins studied in fact constitutes events that are upstream of the step involving Ca_i^{2+} recruitment. BCR engagement leads first to the activation of Src PTKs, which include Lyn and Lck (Campbell and Sefton, 1992; Fuentes-Panana et al., 2004). Activated Lyn then phosphorylates BCR-associated CD79a and CD79b, following which Syk is recruited at these sites. This process constitutes a prerequisite for activation of the downstream signaling components, one of which includes the Syk-dependent phosphorylation and activation of PLCγ. Activated PLCγ cleaves phosphatidylinositol 4,5-bisphosphate (PIP2) to generate IP3 as one of the secondary metabolites. Here the adaptor protein BLNK plays a critical role in both the recruitment of PLCγ2 to the plasma membrane and positioning it in proximity with PIP2 (Kurosaki and Tsukada, 2000). The IP3 thus generated induces Ca_i^{2+} release from the ER.

Our finding that Lyn phosphorylation was Ca^{2+} sensitive (Figure 2) therefore suggested that the effect of Ca_i^{2+} deprivation was likely exercised at a very early step in the BCR signaling pathway. As phosphorylation of Src PTKs, and Lyn in particular, is thought to constitute the initiating event in BCR signaling, it was plausible that this perturbation in Lyn phosphorylation could account for the global effect of Ca_i^{2+} blockage on BCR signaling. Consequently, we next studied the effects of Ca_i^{2+} depletion on activation of the Lyn kinase. Lyn was immunoprecipitated from stimulated cells and its kinase activity measured using an exogenous synthetic-peptide substrate. Stimulation with anti-IgG led to a rapid activation of Lyn kinase that peaked between 1 and 5 min of stimulation time (Figure 3A). Importantly,

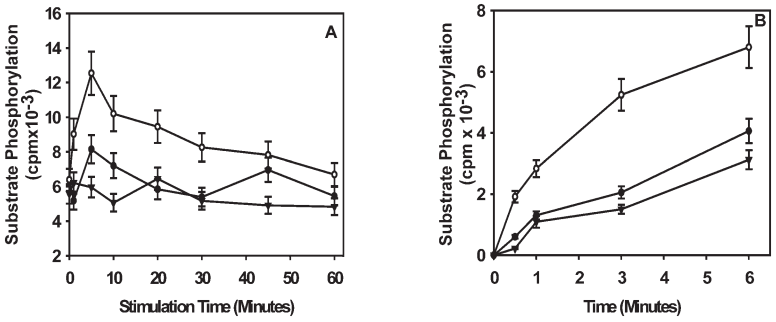

Figure 3. Ca_i^{2+} Deprivation Results in Diminished Activation of Lyn

In (A), Lyn was immunoprecipitated from cells (2 × 10^7/group) stimulated for the indicated times in the absence (○) or presence of either EGTA (●) or TMB-8 (▼). These immunoprecipitates were then employed in a phosphorylation assay using a synthetic peptide as substrate. Results give the net incorporation of radioactive phosphate in the substrate after background subtraction. In (B), untreated cells (○) or cells treated with either EGTA (●) or TMB-8 (▼) were stimulated for 1 min with anti-IgG. The Lyn immunoprecipitates thus obtained were used in a substrate phosphorylation assay where substrate phosphorylation was monitored as a function of time. Values shown represent the time-dependent increase in peptide phosphorylation. In both (A) and (B), values are the mean (±SD) of four experiments where each experiment was performed in triplicate sets.

Lyn activation was severely compromised in samples obtained from cells stimulated in the presence of either EGTA or TMB-8. This was especially evident at the early time points, where the inhibition was again greater with TMB-8 relative to that with EGTA. In addition to the magnitude, Lyn obtained from Ca_i^{2+}-deprived cells also displayed a reduction in the kinetics of substrate phosphorylation (Figure 3B). EGTA treatment resulted in a 5- to 6-fold reduction in the rate of substrate phosphorylation, whereas the difference in the corresponding rates between samples from EGTA- versus TMB-8-treated cells was about 1.4-fold. Thus, the BCR-dependent Ca_i^{2+} response directly regulates the proportion of available Lyn molecules that are activated. This, in turn, regulates both the extent and rate of substrate phosphorylation that is achieved by this kinase.

BCR Engagement Leads to a Ca_i^{2+}-Dependent Generation of ROS

A second messenger function for ROS has been implicated in diverse receptor systems, including those for EGF, PDGF, insulin, and the TCR, among others (Finkel, 2003; Nathan, 2003; Devadas et al., 2002). Signal activation of lymphocyte receptors has been proposed to occur through H_2O_2-mediated inhibition of protein tyrosine phosphatase (PTP) activity, thereby shifting the equilibrium in favor of kinase activation (Reth, 2002; Reth and Brummer, 2004). Therefore, we next probed whether stimulation of A20 cells with anti-IgG results in the production of ROS using cells that were labeled with a ROS-sensitive dye, DCFDA. A rapid induction of ROS was observedthat was evident within seconds of addition of anti-IgG (Figure 4A). This anti-IgG-dependent ROS induction could be inhibited by the addition of either the glutathione peroxidase mimetic ebselen or the antioxidant N-acetylcysteine (NAC) (Figure 4A) but not by the NO scavenger L-N-monomethyl arginine (not shown). Furthermore, overexpression of either catalase or peroxiredoxin 1 (Prdx1)—both of which are known H_2O_2 scavengers—also led to inhibition of the anti-IgG-induced ROS response (Figure 4A). These results cumulatively demonstrate that stimulation of BCR leads to the rapid generation of ROS, which is at least largely comprised of H_2O_2.

Optimal BCR-dependent ROS induction required the prior activation of PTK and PI3K. Inhibition of either the PTK activity with genistein or the PI3K activity with wortmannin led to a significant reduction in anti-IgG-dependent ROS production (Figure 4B). Thus, activation of BCR signaling is required for generation of at least a significant proportion of the ROS detected. BCR-dependent ROS production was also significantly inhibited in the presence of either EGTA (~60%) or TMB-8 (~75%) (Figure 4C). Significantly, this inhibitory effect was exercised at the earliest time points of ROS detection (Figure 4C, inset) and could be reversed under conditions of Ca^{2+} supplementation (Figure S4). Suppressed anti-IgG-dependent ROS responses could also be demonstrated in cells treated with BAPTA-AM and in cells suspended in Ca^{2+}-deficient medium (Figure 4C). These results reveal that the inhibition of BCR-dependent Ca_i^{2+} recruitment results in a concomitant inhibition of the BCR-dependent ROS response.

Consistent with earlier suggestions (Qin et al., 2000; Reth, 2002), we found that suppression of BCR-initiated ROS generation also resulted in an attenuated Ca_i^{2+} response. This could be demonstrated in cells stimulated in the presence of antioxidants such as ebselen or NAC as well as in cells overexpressing either catalase or Prdx1 (Figure 4D). Thus, these cumulative findings identify the existence of a positive feedback loop between the BCR-dependent Ca_i^{2+} and the BCR-dependent ROS responses. Furthermore, the inhibitory effect of EGTA and TMB-8 on the BCR-dependent ROS levels was dose dependent (Figure 4E), as was the effect of ROS scavengers on the BCR-activated Ca_i^{2+} response (Figure 4F). These latter results thus describe the Ca_i^{2+}-ROS loop as a monostable system that can display graded shifts in its steady-state equilibrium. A sigmoidal dose-response curve is expected for bistable systems, whereas incremental effects are characteristic of monostable systems (Ferrell, 2002).

To probe for a regulatory effect of the Ca_i^{2+}-ROS loop, we next examined Lyn phosphorylation after selectively depleting either of these two species. Our interest being in the early signaling events, we focused on the 30 s time point of stimulation with anti-IgG. Both EGTA and TMB-8 led to a marked reduction in inducible Lyn phosphorylation, which could be reversed by Ca^{2+} supplementation (Figure 5A). A similar effect was noted in cells that were either treated with BAPTA-AM or suspended in medium that was deficient for Ca^{2+} prior to stimulation (Figure 5A), further confirming a role for

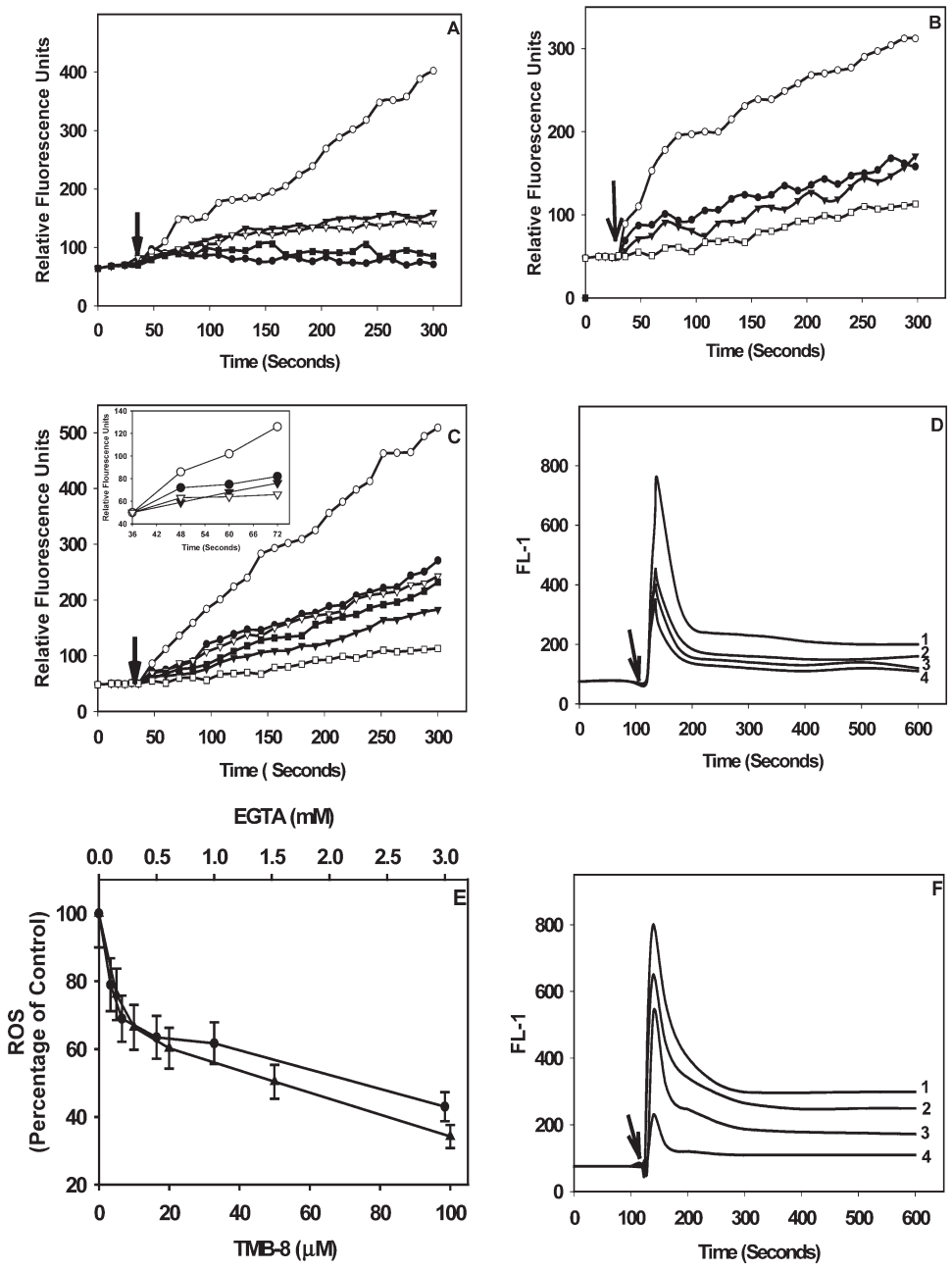

Figure 4. Cooperativity between Ca_i^{2+} and ROS Pathways

(A)–(C) profile the generation of ROS as measured by DCFDA oxidation. Briefly, DCFDA-labeled A20 cells were plated at 1 × 10^6/100 μl in wells of a 96-well plate, and the fluorescence signal obtained after stimulation with anti-IgG under the various conditions employed was recorded for the periods shown. Results for cells stimulated with anti-IgG in the absence of any inhibitor (○) are shown in all panels. In (B) and (C), the profile for mock-stimulated (i.e., medium-only) cells is also included (□). The arrow indicates the time of addition of anti-IgG. (A) gives the results for cells stimulated with anti-IgG in the presence of either 15 mM ebselen (■) or 25 mM NAC (●) or in cells transfected with either catalase (▽) or Prdx1 (▼). The profile obtained upon stimulation of mock-transfected (i.e., vector-only) cells did not differ significantly from that in untransfected cells. Values shown are after subtracting the corresponding values for mock-stimulated cells at each of these time points. (B) depicts ROS in cells stimulated with anti-IgG in presence of either 100 nM wortmannin (●) or 50 μg/ml of genistein (▼). (C) shows ROS production in cells stimulated in the presence of either 3 mM EGTA (●), 5 mM BAPTA-AM (■), or 100 mM TMB-8 (▼) or suspended in Ca^{2+}-free medium prior to stimulation (▽). The inset compares profiles obtained with EGTA, TMB-8, or BAPTA-AM and cells stimulated without inhibitor within the first 36 s after anti-IgG addition. (D) depicts the Ca_i^{2+} responses in Fluo-3-AM-loaded A20 cells stimulated either alone (line 1) or in the presence of 10 mM NAC (line 2) or in cells overexpressing either Prdx1 (line 3) or catalase (line 4). (E) shows the dose-dependent inhibition of anti-IgG-stimulated ROS generation in response to increasing doses of either TMB-8 (▲) or EGTA (●); data given are the mean (±SD) of four separate experiments. (F) shows the dose-dependent inhibition of the Ca_i^{2+} response by ebselen as monitored by FACS. Fluo-3-AM-loaded cells were stimulated with anti-IgG in the absence (line 1) or presence of 2 mM (line 2), 5 mM (line 3), or 15 mM (line 4) ebselen.

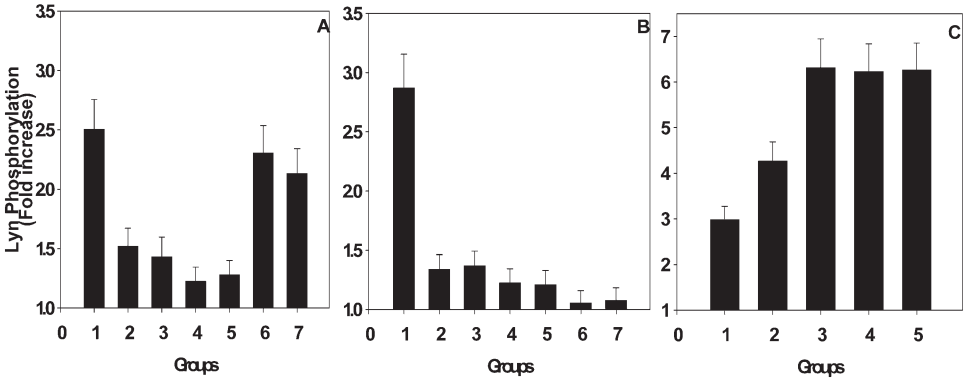

Figure 5. The Effect of Ca_i^{2+} on Lyn Phosphorylation Is Mediated through ROS

Lyn immunoprecipitation was done from cells stimulated for 30 s under different conditions and probed for phosphotyrosine. Lyn phosphorylation was quantified by densitometry; values are presented as fold increase over that obtained for Lyn in mock-stimulated cells. In (A), group 1 represents cells stimulated with anti-IgG. Groups 3–7 represent cells stimulated with anti-IgG in the presence of EGTA, TMB-8, BAPTA-AM, EGTA plus $CaCl_2$, and TMB-8 plus ionomycin, respectively. Group 2 shows the results obtained in cells suspended in Ca^{2+}-free medium. (B) gives the corresponding results obtained in cells treated with either ebselen (group 2), ebselen plus ionomycin (group 3), NAC (group 4), or NAC plus ionomycin (group 5). Data for cells overexpressing either catalase (group 6) or Prdx1 (group 7) are also shown, along with the corresponding values obtained in mock-transfected cells (group 1). (C) shows the effect of stimulation of cells with either anti-IgG (group 1), H_2O_2 (group 2), or sodium pervanadate (group 3). The consequences of stimulation with sodium pervanadate in the presence of either EGTA (group 4) or TMB-8 (group 5) are also depicted. Values shown in (A)–(C) are the mean (±SD) of three independent experiments.

Ca_i^{2+} in regulating BCR-dependent Lyn phosphorylation.

The H_2O_2 scavengers ebselen and NAC were equally capable of inhibiting BCR-dependent Lyn phosphorylation, as was the overexpression of either catalase or Prdx1 (Figure 5B). The addition of ionomycin, however, had no effect on this inhibition, suggesting a redundancy of Ca_i^{2+} in this process. Consistent with a role for ROS in Lyn phosphorylation, addition of either H_2O_2 or pervanadate to A20 cells also led to enhanced phosphorylation of Lyn (Figure 5C). While exogenous ROS is known to induce Ca_i^{2+} recruitment in B cells (Reth, 2002), this effect was not inhibited by the addition of either EGTA or TMB-8 (Figure 5C). These results, therefore, highlight a regulatory role for the Ca_i^{2+}-ROS loop during BCR-dependent phosphorylation of Lyn. Furthermore, our demonstration that Lyn phosphorylation was insensitive to the effects of Ca_i^{2+} depletion in the presence of exogenous ROS, combined with the fact that Ca^{2+} supplementation was unable to alleviate the inhibitory effects of ROS scavengers, reveals that it is the ROS that directly mediates this effect. The Ca_i^{2+} then likely influences the levels of ROS available. This interpretation is consistent with our findings that inclusion of ebselen during stimulation of cells with anti-IgG also leads to a global dampening of BCR signals (Figure S5).

The Ca_i^{2+}-ROS Loop Regulates Phosphatase Activities Associated with the BCR

A likely target candidate for the action of ROS are the PTPs, which have a redox-regulated cysteine in their catalytic site (Zhang, 1998; Reth, 2002). As the effect of ROS suppression was evidenced at the level of Lyn phosphorylation, we anticipated that the putative target PTP would be one that is either in close proximity to or associated with the BCR. The association of the PTP SHP-1 with the BCR has previously been demonstrated in murine B cells, and a deficiency in SHP-1 activity was correlated with hyperresponsiveness to BCR stimulation in terms of both proliferation and intracellular signaling (Pani et al., 1995). Experiments involving sIgG immunoprecipitations followed by a Western blot analysis also confirmed the association of SHP-1 with the BCR in A20 cells. This association was stable to the effects of BCR stimulation and was resistant to the effects of either EGTA or TMB-8 addition (Figure 6A). The association of SHP-1 with the BCR was further confirmed through mass spectrometric analysis of tryptic digests generated from the immunoprecipitates obtained from unstimulated cells (data not shown). The latter experiments failed to reveal the presence of any additional PTP, suggesting that SHP-1 constitutes at least the predominant PTP associated with the BCR.

We next monitored BCR-associated PTP activity as a function of stimulation time. A rapid but transient inactivation was observed in samples from cells stimulated in the absence of any added inhibitor (Figure 6B). Inhibition was detected by 15 s after stimulation, with maximal levels (~60% inhibition) being achieved at 30 s. Surprisingly, the PTP activity was then rapidly restored to slightly above basal levels by 1 min and remained relatively invariant thereafter (Figure 6B). Addition of either EGTA or TMB-8 prevented this inhibition, with TMB-8 in fact yielding an enhancement in PTP activity at the early time points (Figure 6B).

Addition of the ROS scavengers ebselen or NAC also led to a complete suppression of BCR-associated PTP inactivation induced by anti-IgG (Figure 6C), which was similar to the effects of overexpression of either catalase or Prdx1 (Figure 6C). That the observed PTP inactivation was mediated by ROS could be confirmed in additional experiments employing pervanadate as the stimulant instead of anti-IgG. An inhibition profile sim-

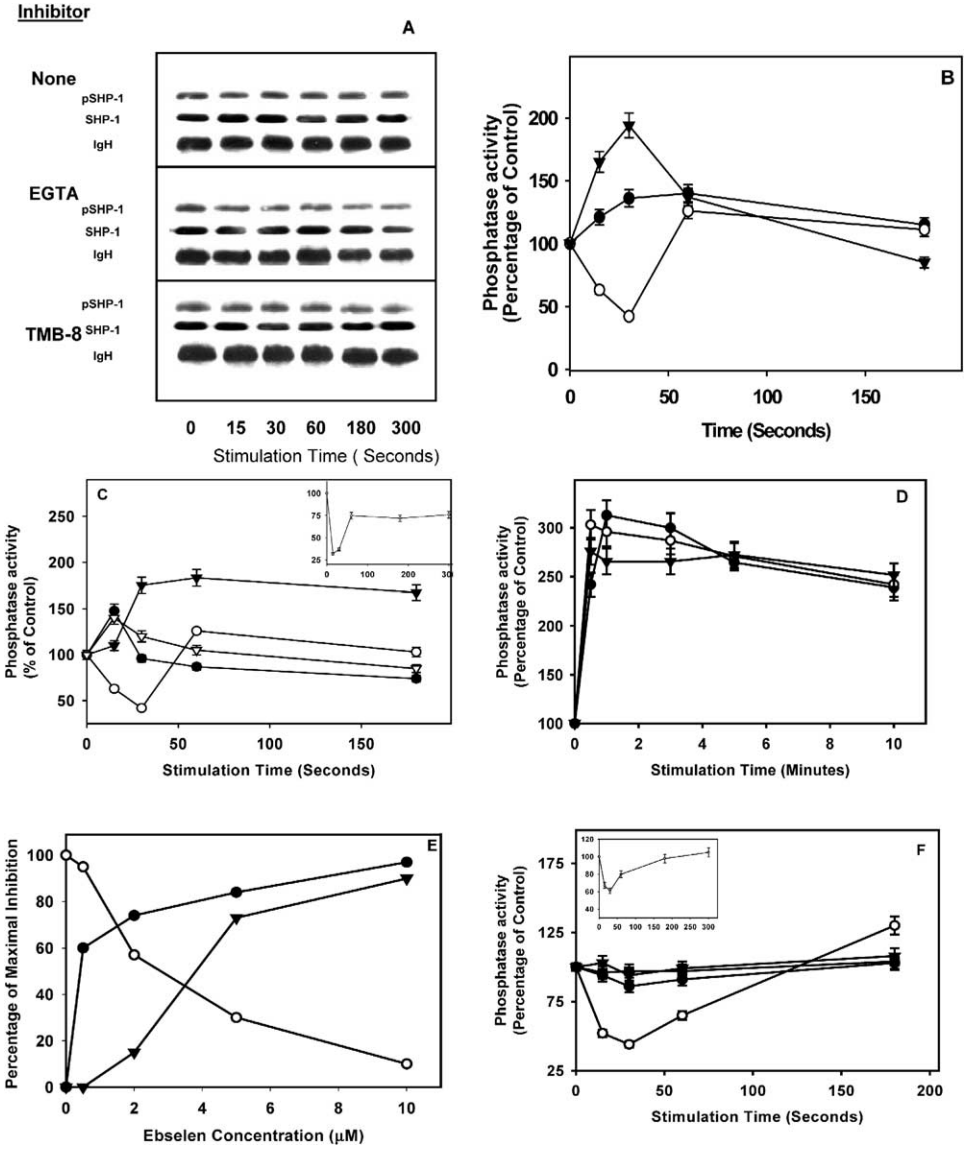

Figure 6. The Ca_i^{2+}-ROS Loop Regulates BCR-Associated PTP Activity

Cells (5×10^7/aliquot) were stimulated with anti-IgG in the presence or absence of various inhibitors for the times indicated. Cell lysates were then subjected to immunoprecipitation with either anti-mouse IgG (A–C) or anti-B220 (B cell-specific isoform of CD45) antibodies (F). (A) shows the Western blot results when immunoprecipitates from the various groups were probed for either the Ig heavy chain (IgH, as loading control) or the presence of SHP-1. The SHP-1 blots were then stripped free of bound antibody and reprobed with anti-phosphotyrosine antibodies (pSHP-1). In (B) and (C) an identical protocol was employed, except that the immunoprecipitates were employed in an assay for detecting phosphatase activity. Profiles shown in (B) are for cells stimulated in the absence (○) or presence of either EGTA (●) or TMB-8 (▼). (C) gives the corresponding results obtained in either mock-transfected cells (○), cells transfected with a vector coding for Prdx1 (●) or catalase (▼), or the presence of ebselen (▽). Inset shows the results obtained upon stimulation of cells with pervanadate instead of anti-IgG. The supernatants remaining after sIgG-immunoprecipitation were subjected to a second round of immunoprecipitation with anti-SHP-1 antibodies. Results of a phosphatase-activity assay on this precipitate are shown in (D). The groups are cells stimulated in the absence (○) or presence of either ebselen (●) or TMB-8 (▼). (E) depicts the effects of increasing ebselen concentrations at 30 s of anti-IgG stimulation on BCR-associated PTP activity (○), BCR-dependent ROS production (●), and BCR-dependent Lyn phosphorylation (▼) in A20 cells. For comparison, values are normalized in terms of percent of the maximal inhibition obtained (i.e., anti-IgG alone for PTP activity and 20 mM ebselen for ROS and Lyn phosphorylation). (F) depicts the phosphatase activity obtained from CD45 (or B220) immunoprecipitates. The various groups are cells stimulated without an inhibitor (○) or with either EGTA (●), TMB-8 (▼), or ebselen (▽). Inset shows the effect on the activity of CD45 of stimulating cells with pervanadate. No additional effect was detected here upon addition of either EGTA or TMB-8. Data presented in (B)–(F) are the mean (±SD for [B]–[D]) of between three and five experiments.

ilar to that of anti-IgG was obtained (Figure 6C, inset), although neither EGTA nor TMB-8 addition was able to overcome the inhibition in this case. These results indicate that it is the BCR-initiated ROS that is directly involved in the transient inhibition of BCR-associated PTP activity, the latter probably deriving from SHP-1.

The anti-IgG-induced inhibition of BCR-associated PTP activity was reversed simply by incubation of the immunoprecipitates for a brief period with DTT (data not shown), supporting that inactivation involved reversible oxidation of a cysteine residue in the PTP. Importantly, anti-IgG-mediated inhibition of PTP activity was found to be restricted to the BCR-associated pool of SHP-1. No inhibitory effect could be detected on SHP-1 that was directly immunoprecipitated from cell lysates that had been first depleted of the BCR (Figure 6D). Rather, an increase in activity was observed that was not further affected upon addition of either Ca_i^{2+} or ROS inhibitors (Figure 6D). Thus, it appears that the action of ROS is specific to the BCR-associated SHP-1.

A direct correlation between available ROS concentrations, the consequent inactivation of BCR-associated PTP, and BCR-dependent Lyn phosphorylation could be verified in experiments using ebselen as an exogenous ROS inhibitor. Stimulation of cells with anti-IgG in the presence of increasing ebselen concentrations led to a dose-dependent inhibition in ROS production (Figure 6E). Importantly, this also resulted in a corresponding dose-dependent reduction in the extent of PTP inactivation along with a progressive decrease in BCR-dependent Lyn phosphorylation (Figure 6E). These findings provide experimental support for our proposal that the Ca_i^{2+}-ROS loop represents a monostable system that is capable of calibrating signal output from the BCR.

In addition to the effect on BCR-associated PTP activity, stimulation of A20 cells with anti-IgG also resulted in a rapid but transient inactivation of CD45 (B220), a transmembrane PTP that plays a critical role in controlling BCR signal transduction (Alexander, 2000) (Figure 6F). Stimulation of cells in the presence of inhibitors of either Ca_i^{2+} or ROS led to a reversal of this inhibition (Figure 6F). Furthermore, a similar inhibition in CD45 activity was also obtained upon stimulation with sodium pervanadate instead of anti-IgG, and this inhibitory effect was now insensitive to both EGTA and TMB-8 (Figure 6F, inset). Thus, in addition to the BCR-associated PTP, the Ca_i^{2+}-ROS feedback loop also appears to regulate enzymatic activity of CD45 in a ROS-dependent manner.

BCR-Dependent ROS Production Is Mediated through *DUOX1*

While the enzymatic component responsible for BCR-dependent ROS generation remained unknown, NADPH oxidases (NOX) have been implicated for a variety of receptors, including the TCR (Jackson et al., 2004). To test for such a possibility, we next stimulated cells in the presence of a flavin-dependent oxygenase inhibitor, diphenylene iodonium (DPI). This treatment resulted in a significant inhibition of the early BCR-dependent ROS response (Figure 7A). Importantly, the inclusion of DPI during stimulation significantly inhibited the BCR- but not the H_2O_2-dependent phosphorylation of Lyn (Figure 7B), implicating the involvement of an NADPH oxidase in at least some of the early BCR-dependent H_2O_2 production.

Of the NOX family members, it is the human NOX5 that is regulated by cytosolic Ca^{2+} concentrations (Banfi et al., 2004). However, such Ca_i^{2+}-regulated NOX members have not yet been described in mice. Furthermore, a comparison of the sequence of the human NOX5 (*hNOX5*) gene against the mouse genome database also did not identify any closely related homologs. However, an annotated murine cDNA sequence identified as *DUOX1* (accession number XM_130483.4) was discovered that displayed 87% sequence identity with that of its human DUOX (dual oxidases) counterpart. DUOX represents the second family of nonphagocytic NADPH oxidases that depend upon either $gp91^{phox}$ or its related proteins (Lambeth et al., 2000). This class of enzymes possesses two EF hand motifs, and Ca_i^{2+}-activated superoxide production has previously been suggested for the human homologs (Nakamura et al., 1991; Banfi et al., 2001).

Thus, in the absence of a murine NOX5 homolog, *DUOX1* seemed a likely candidate to be involved in BCR-dependent ROS production. Our subsequent experiments revealed that *DUOX1* was indeed expressed in A20 cells, in addition to a few other B cell lines and normal mouse splenic B cells. This was confirmed both by Northern blot hybridization and reverse transcriptase-PCR experiments with isolated mRNA (Figure S6).

To examine the role of *DUOX1*, we next performed gene-silencing experiments using a combination of double-stranded siRNAs targeting two nonoverlapping regions from the annotated cDNA sequence of the *DUOX1* gene. This approach led to a substantial reduction in the specific mRNA levels by 48 hr posttransfection (Figure 7C). Significantly, suppression of *DUOX1* expression led to a concomitant inhibition of the early ROS response that is obtained upon BCR triggering (Figure 7D). No such inhibition could be observed in the negative control where cells were transfected with nonsilencing oligonucleotide sequences (Figure 7D). In addition to ROS, the BCR-dependent Ca_i^{2+} response was also markedly attenuated in cells transfected with the silencing, but not the control, siRNA (Figure 7E). Finally, BCR-dependent phosphorylation of Lyn was also negatively affected in cells displaying reduced *DUOX1* expression (Figure 7F). These results, therefore, strongly implicate *DUOX1* as constituting at least one of the components responsible for the early phase of the BCR-dependent ROS response. Thus, it is the *DUOX1*-mediated ROS that appears to be involved in establishing the Ca_i^{2+}-ROS feedback loop and, thereby, influencing BCR-dependent Lyn phosphorylation.

Discussion

While Ca_i^{2+} is known to drive several downstream pathways (Winslow et al., 2003), the global dampening of BCR signaling seen upon inhibition of Ca_i^{2+} was unexpected. At least within the time frame of our experiment, the signals emanating upon BCR activation could be differentiated into two sequential peaks of phosphorylation that occurred at 1 min and 10 min of stimulation, respectively. Interestingly, both of these phases were significantly attenuated when BCR-dependent Ca_i^{2+} mobilization was inhibited with either EGTA or TMB-8. However, the graded inhibitory effect, depending on whether Ca_i^{2+} blockage was complete or merely

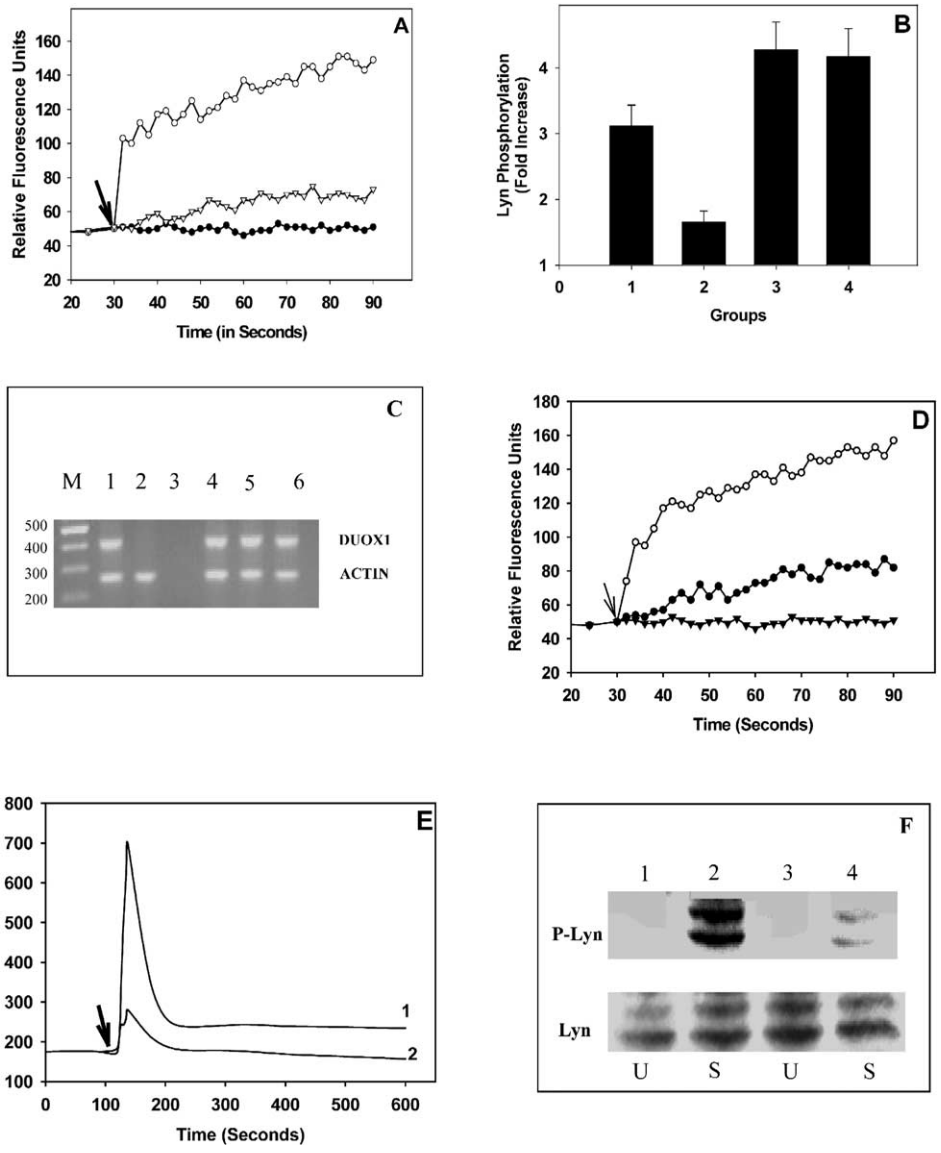

Figure 7. The *DUOX1* Gene Product Mediates BCR-Dependent ROS Generation

DCFDA-labeled A20 cells were stimulated with anti-IgG in the absence (○) or presence of DPI (15 μM, ▽); the resulting increase in the fluorescence signal obtained over a subsequent 60 s period is shown in (A). Also included here is the profile obtained in unstimulated cells (●). (B) depicts the fold increase in Lyn phosphorylation in cells stimulated with either anti-IgG (groups 1 and 2) or H_2O_2 (groups 3 and 4) in the absence (groups 1 and 3) or presence (groups 2 and 4) of DPI. Values are the mean (± SD) of three independent experiments. (C) shows the results of a semiquantitative RT-PCR analysis of total RNA obtained, 48 hr later, from cells transfected with either silencing (lane 2) or nonsilencing (lanes 4 to 6) siRNA. Nonsilencing siRNA was targeted against either aminopeptidase-N from *Spodoptera litura* (lane 4), luciferase (lane 5), or murine SMAR-1 (lane 6). *DUOX1* expression in cells prior to siRNA treatment is shown in lane 1. Parallel PCR was also done on the mRNA preparation from A20 cells after omitting the reverse transcriptase reaction to verify that contaminating genomic DNA was not being amplified (lane 3). (D) shows the early anti-IgG-induced ROS responses obtained in cells that were transfected with either *DUOX1*-silencing (●) or nonsilencing (○) siRNA. Also included is the corresponding profile obtained in unstimulated cells (▼). (E) profiles the corresponding BCR-dependent Ca_i^{2+} response (line 1, negative control; line 2, *DUOX1*-silenced cells). Lyn phosphorylation (P-Lyn) obtained is shown in (F) in cells that were transfected with either irrelevant (lanes 1 and 2) or silencing (lanes 3 and 4) siRNA in either the presence (S) or absence (U) of 1 min stimulation with anti-IgG. These blots were subsequently stripped and reprobed with antibodies specific for the Lyn protein (Lyn) to verify comparable protein load in the lanes.

restricted to the CCE phase, proved to be particularly informative. Addition of TMB-8 during stimulation caused a severe attenuation in the primary phase of signaling, as a result of which the second phase was virtually undetectable. As opposed to this, selective inhibition of CCE with EGTA led to a less severe inhibition in the first peak of signaling but was accompanied by a time lag in the generation of the second peak. At least on an empirical level, these collective findings permit two important inferences to be drawn. First, the strength of

the initial signal generated influences the extent to which it eventually progresses. This interpretation is supported by our observations that the extent of inhibition of the primary phosphorylation events determined the intensity of the latter phase. Second, the strength of the initial signal generated also likely determines the subsequent rate of signal progression. This was evident in the intermediate situation of CCE blockage, where time lags in signal accumulation were noted. Our proposal that both the extent and rate of signal progression depend upon the amplitude of the initial signal is easily rationalized simply by considering the law of mass action. Thus, in any sequential process the concentration of the active intermediate generated at any given step may be expected to determine the facility, in terms of both magnitude and rate, with which the subsequent step will occur.

From a mechanistic point of view, it was intriguing that the effect of Ca_i^{2+} was enforced at a point in the pathway that preceded the initiation of BCR signaling (Lyn phosphorylation). Experimental support for this feedback interaction revealed to us the framework within which BCR signal amplification could be achieved. This was visualized as follows: ligation of the BCR first leads to a relatively low-intensity activation of BCR signaling; the Ca_i^{2+} thus recruited rapidly establishes a self-sustaining feedback loop that leads to signal amplification from its point of origin. Our results indicate that this feedback cooperativity is instituted at least within seconds of BCR activation. Subsequent resolution revealed that Ca_i^{2+} acted by potentiating BCR-dependent production of ROS. A positive cooperativity between the BCR-dependent Ca_i^{2+} and the BCR-dependent ROS pathways was indeed identified in which inhibition of one led to a concomitant inhibition of the other.

The predominant oxidant species produced in response to stimulation of A20 cells with anti-IgG appears to be H_2O_2, at least as deduced from the experiments described here. Importantly, ROS was rapidly induced, being detectable within seconds of addition of anti-IgG. Furthermore, the effect of Ca_i^{2+} on ROS levels was also evident from the earliest time point of detection of ROS. In this context our present results identify *DUOX1* as at least one of the enzymatic components responsible for the early BCR-dependent ROS production. Our experiments employing siRNA revealed that *DUOX1* is critical for establishing the BCR-dependent Ca_i^{2+}-ROS feedback loop and, thereby, ensuring optimal phosphorylation of Lyn following BCR activation.

While both the BCR-dependent Ca_i^{2+} and ROS pathways influenced each other, it was the ROS that ultimately affected BCR signaling. This was determined from experiments indicating that, whereas the inhibitory effect of Ca_i^{2+} could be overcome by independent elevation in ROS levels, the converse was not true. Furthermore, the effect of ROS suppression was evident at the level of Lyn phosphorylation, as a result of which both the magnitude and kinetics of substrate phosphorylation by Lyn were attenuated. Since Lyn—along with the other Src kinases—constitutes the initiating event in BCR signaling, we speculate that it is the effect of ROS on Lyn activation that then impacts the subsequent signaling events.

The ROS produced upon BCR activation was found to act through inhibition of PTPs. Notable here was the effect on BCR-associated SHP-1, where the inhibition was spatially localized with no effect on the cytoplasmic pool of SHP-1. A similar inhibition was also obtained for CD45, a transmembrane PTP involved in the regulation of BCR signaling. Importantly, ROS-mediated inactivation of PTP was in turn regulated through the receptor-initiated recruitment of Ca_i^{2+}. In view of the fact that the ROS production upon BCR activation was relatively stable, the transient inhibition of PTP activity obtained was, however, somewhat surprising. While the reason for this is not presently clear, more recent experiments have determined the antioxidant protein peroxiredoxin 4 (Prdx4) to be associated with the BCR (Figure S7). Whether such BCR-associated antioxidant proteins in fact regulate ROS-mediated PTP inhibition, however, remains to be established. In any event, a similar transient PTP inactivation was obtained when cells were stimulated with pervanadate instead of anti-IgG. More importantly, short-lived ROS-mediated PTP inhibition has also been noted during activation of other receptor systems (Lee et al., 1998; Mahadev et al., 2001; Meng et al., 2002). Collectively, then, our present results, along with these earlier findings, strongly suggest that a pulsed inactivation of the receptor-coupled PTP is sufficient to shift the balance in favor of signal activation. In this context we consider it likely that, by varying the extent of PTP inactivation, the Ca_i^{2+}-ROS loop acquires a rheostat-like function in terms of modulating the strength of BCR signaling. This is based on our description of this loop as a monostable system, along with the fact that additional pathways that control the concentrations of Ca_i^{2+} and ROS produced in response to BCR triggering have recently been characterized (Nishida et al., 2003; Saito et al., 2003). That calibrated shifts in the Ca_i^{2+}-ROS equilibrium can lead to a graded output is experimentally supported by our demonstration of the dose-dependent correlation between ROS concentrations available, the extent of inactivation of the BCR-associated PTP, and the magnitude of BCR-dependent Lyn phosphorylation. In other words, it is the Ca_i^{2+}-ROS feedback loop that likely determines the dimensions of time and space in terms of propagation of the BCR-generated signals.

In summary, we identify here the existence of a positive feedback loop between receptor activation-dependent Ca_i^{2+} and ROS that regulates BCR signal strength right at its point of origin. The central nature of this loop was revealed from the fact that its perturbation led to a global dampening of signals. Our results further suggest that it is the strength of the initial signal that determines the extent to which it progresses, in addition to the speed with which the endpoint is reached. Finally, we also characterize the Ca_i^{2+}-ROS loop as a monostable system. This property would enable a rheostat-like function for this loop, with feeder pathways likely to confer on it a "tuning" capability with respect to BCR signal amplification. Finally, given the common usage of both Ca_i^{2+} and ROS as second messengers, it would be of interest to determine whether such a Ca_i^{2+}-ROS

feedback loop also acts during signaling from other receptor systems.

Experimental Procedures

Stimulation of Cells and the Resolution of Phosphorylated Proteins by 2-DE

A20 cells (2×10^7) were placed in phosphate-free DMEM supplemented with 1% FCS for 2 hr, following which [^{32}P]-orthophosphoric acid (0.5 mCi/ml) was added and the culture continued for an additional 4–5 hr. They were then stimulated with the $F(ab)_2$ fragment of goat anti-mouse IgG at a final concentration of 25 μg/ml for the indicated times. Where necessary, the appropriate inhibitor was added at 10 min prior to stimulation (EGTA and TMB-8 at final concentrations of 3 mM and 100 μM, respectively). The cytoplasmic fractions of cell lysates were then resolved by 2-DE as previously described (Gorg et al., 2000). Resolution in the first dimension was achieved using 13 cm IPG dry strips (pH 4–7), and a 12% SDS polyacrylamide gel was used to resolve in the second dimension. Comparable loading in all the groups was ensured through silver staining of the resultant gels. Dried gels were then exposed to X-ray films.

Phosphoproteins were visualized by autoradiography and digitized on a Molecular Dynamics computing densitometer using ImageQuant software (Amersham Biosciences). Only those spots with an area greater than 75 pixels were considered, and the minimum intensity surrounding the spot on the film was taken as its background and subtracted to give the true intensity. Relative quantification was achieved by normalizing against three distinct spots that were unaffected upon anti-IgG stimulation of cells. Calibration for the Mw and pI was done on the basis of standard markers that were run on parallel gels.

Transfection of Cells

The gene for human Cu/Zn superoxide dismutase was a generous gift from J. Subramanium (IIT Kanpur, India), that for mouse Prdx1 from S. Watabe (Yamaguchi University, Japan), and that for EhCaBP from S. Sopory (ICGEB, India). The human catalase gene was obtained by RT-PCR. Each of these genes was cloned into an appropriate series of the mammalian expression vector pcDNA3.1-Myc/His (Invitrogen). Linearized plasmid DNA (20 μg) was transfected by electroporation (260 V, 950 μF) of A20 cells (2×10^7) followed by selection in a medium containing G418 (1.2 mg/ml). Experiments were done at 3 days posttransfection, and parallel transfections were performed with the *lacZ* gene as a positive control. High expression of the Myc/His-tagged proteins was confirmed through Western blot using tag-specific antibodies.

siRNA

A combination of two 21-mer siRNA duplexes specific to the annotated cDNA sequence of *DUOX1* with two-nucleotide (dT) 3′ overhangs was used to downregulate *DUOX1* expression (target sequences: TTGAGACAAAGTGAGAATTAA and GAGCACTGTTTAAGA ACTATA). Each siRNA duplex was used at 10 μg/5×10^6 cells, and transfection was achieved using the RNAiFect kit (Qiagen) and strictly following the protocol recommended by the manufacturer. The negative-control siRNAs used are described in the legend to Figure 7. After 2 days in culture, cells were harvested and then analyzed for the various parameters described in the text.

Lyn Kinase Assay

Lyn was first immunoprecipitated from the various groups (5×10^7 cells/group/time point) described in the text. The immunoprecipitates were washed and then incubated in the kinase reaction buffer (25 mM Tris [pH 7.5] containing 0.5 mM DTT, 0.1 mM orthovanadate, 50 μM unlabeled ATP, 10 mM $MgCl_2$, and 10 μCi/tube of [^{32}P]-ATP). The reaction was initiated through the addition of a 5 μM final concentration of the synthetic-peptide substrate (sequence: AEEEIYGEFEAKKKK). The reaction was terminated by centrifugation followed by spotting 20 μl of the supernatant onto Whatman-81 chromatography paper. After extensive washing, the radioactivity associated with the spots was determined by scintillation counting. To ensure that the results obtained do not reflect variations in the amount of Lyn in the different groups, parallel sets of immunoprecipitates were also analyzed by Western blot using anti-Lyn antibodies. Comparable Lyn-specific band intensities were obtained in these experiments.

Phosphatase Assay

This was done essentially as described earlier, using paranitrophenyl phosphate as the substrate (Hua et al., 1998; Yoshida and Kufe, 2001). That comparable amounts of either SHP-1 or B220 were present in the various tubes was again ensured through Western blot on parallel sets of immunoprecipitates.

Supplemental Data

Supplemental Data include seven figures and are available with this article online at http://www.cell.com/cg/content/full/121/2/281/DC1/.

Acknowledgments

This work was funded by a grant from the Indian Council of Medical Research. D.K.S. and D.K. are recipients of the Shyama Prasad Mukherjee Fellowship and S.K.B. a Senior Research Fellowship, both from the Council of Scientific and Industrial Research. We thank J. Subramanium for a gift of the Cu/Zn SOD-encoding plasmid, S. Watabe for the plasmid encoding Prdx1, and S. Sopory for the plasmid containing the EhCaBP gene. We are also grateful to Dinakar Salunke for synthesis of the Lyn substrate peptide and to Manish Sharma for help with cloning and transfection experiments.

Received: April 20, 2004
Revised: December 20, 2004
Accepted: February 4, 2005
Published: April 21, 2005

References

Alexander, D.R. (2000). The CD45 tyrosine phosphatase: a positive and negative regulator of immune cell function. Semin. Immunol. *12*, 349–359.

Banfi, B., Molnar, G., Maturana, A., Steger, K., Hegedus, B., Demaurex, N., and Krause, K.-H. (2001). A Ca^{2+}-activated NADPH oxidase in testis, spleen and lymph nodes. J. Biol. Chem. *276*, 37594–37601.

Banfi, B., Tirone, F., Durussel, I., Knisz, J., Moskwa, P., Molnar, G.Z., Krause, K.H., and Cox, J.A. (2004). Mechanism of Ca^{2+} activation of the NADPH oxidase 5 (NOX5). J. Biol. Chem. *279*, 18583–18591.

Bhalla, U.S., and Iyengar, R. (1999). Emergent properties of networks of biological signaling pathways. Science *283*, 381–387.

Campbell, M.A., and Sefton, B.M. (1992). Association between B-lymphocyte membrane immunoglobulin and multiple members of the Src family of protein tyrosine kinases. Mol. Cell. Biol. *12*, 2315–2321.

Devadas, S., Zaritskaya, L., Rhee, S.G., Oberley, L., and Williams, M.S. (2002). Discrete generation of superoxide and hydrogen peroxide by T cell receptor stimulation: selective regulation of mitogen-activated protein kinase activation and fas ligand expression. J. Exp. Med. *195*, 59–70.

Dolmetsch, R.F., Xu, F., and Lewis, R. (1998). Calcium oscillations increase the efficiency and specificity of gene expression. Nature *392*, 933–936.

Ferrell, E.F., Jr. (2002). Self-perpetuating states in signal transduction: positive feedback, double-negative feedback and bistability. Curr. Opin. Chem. Biol. *6*, 140–148.

Finkel, T. (2003). Oxidant signals and oxidative stress. Curr. Opin. Cell Biol. *15*, 247–254.

Fuentes-Panana, E.M., Bannish, G., and Monroe, J.G. (2004). Basal B-cell receptor signaling in B lymphocytes: mechanisms of regulation and role in positive selection, differentiation and peripheral survival. Immunol. Rev. *197*, 26–40.

Gorg, A., Obermaier, C., Boguth, G., Harder, A., Scheibe, B., Wild-

gruber, R., and Weiss, W. (2000). The current state of two-dimensional electrophoresis with immobilized pH gradients. Electrophoresis *21*, 1037–1053.

Heinrich, R., Neel, B.G., and Rapoport, T.A. (2002). Mathematical models of protein kinase signal transduction. Mol. Cell *9*, 957–970.

Hua, C.T., Gamble, J.R., Vadas, M.A., and Jackson, D.E. (1998). Recruitment and activation of SHP-1 protein tyrosine-phosphatase by human endothelial cell adhesion molecule-1 (PECAM-1). J. Biol. Chem. *273*, 28332–28340.

Jackson, S.H., Devadas, S., Kwon, J., Pinto, L.A., and Williams, M.S. (2004). T cells express a phagocyte-type NADPH oxidase that is activated after T cell receptor stimulation. Nat. Immunol. *5*, 818–827.

Kubohara, Y., and Hosaka, K. (1999). The putative morphogen, DIF-1, of *Dictyostelium discoideum* activates Akt/PKB in human leukemia K562 cells. Biochem. Biophys. Res. Commun. *263*, 790–793.

Kurosaki, T. (2002). Regulation of B cell fates by BCR signaling components. Curr. Opin. Immunol. *14*, 341–347.

Kurosaki, T., and Tsukada, S. (2000). BLNK: connecting Syk and Btk to calcium signals. Immunity *12*, 1–5.

Lambeth, J.D., Cheng, G., Arnold, R.S., and Edens, W.A. (2000). Novel homologs of gp91phox. Trends Biochem. Sci. *25*, 459–461.

Lee, S.-R., Kwon, K.-S., Kim, S.-R., and Rhee, S.G. (1998). Reversible inactivation of protein-tyrosine phosphatase 1B in A431 cells stimulated with epidermal growth factor. J. Biol. Chem. *273*, 15366–15372.

Mahadev, K., Zilbering, A., Zhu, L., and Goldstein, B.J. (2001). Insulin-stimulated hydrogen peroxide reversibly inhibits protein-tyrosine phosphatase 1B in vivo and enhances the early insulin action cascade. J. Biol. Chem. *276*, 21938–21942.

Meng, T.-C., Fukada, T., and Tonks, N.K. (2002). Reversible oxidation and inactivation of protein tyrosine phosphatases in vivo. Mol. Cell *9*, 387–399.

Nakamura, Y., Makino, R., Tanaka, T., Ishimura, Y., and Ohtaki, S. (1991). Mechanism of H_2O_2 production in porcine thyroid cells. Biochemistry *30*, 4880–4886.

Nathan, C. (2003). Specificity of a third kind: reactive oxygen and nitrogen intermediates in cell signaling. J. Clin. Invest. *111*, 769–778.

Nishida, M., Sugimoto, K., Hara, Y., Morii, T., Kurosaki, T., and Mori, Y. (2003). Amplification of receptor signaling by Ca^{2+} entry-mediated translocation and activation of PLCγ2 in B lymphocytes. EMBO J. *22*, 4677–4688.

Pani, G., Kozlowski, M., Cambier, J.C., Mills, G.B., and Siminovitch, K.A. (1995). Identification of the tyrosine phosphatase PTP1C as a B cell antigen receptor-associated protein involved in the regulation of B cell signaling. J. Exp. Med. *181*, 2077–2084.

Pawson, T., and Saxton, T.M. (1999). Signaling networks—do all roads lead to the same genes? Cell *97*, 675–678.

Pawson, T., and Scott, J.D. (1997). Signaling through scaffolding, anchoring and adaptor proteins. Science *278*, 2075–2080.

Qin, S., Stadtman, E.R., and Chock, P.B. (2000). Regulation of oxidative stress-induced calcium release by phosphatidylinositol 3-kinase and Bruton's tyrosine kinase in B cells. Proc. Natl. Acad. Sci. USA *97*, 7118–7123.

Reth, M. (2002). Hydrogen peroxide as a second messenger in lymphocyte activation. Nat. Immunol. *3*, 1129–1134.

Reth, M., and Brummer, T. (2004). Feedback regulation of lymphocyte signalling. Nat. Rev. Immunol. *4*, 269–277.

Saito, K., Tolias, K.F., Saci, A., Koon, H.B., Humphries, L.A., Scharenberg, A., Rawlings, D.J., Kinet, J.-P., and Carpenter, C.J. (2003). BTK regulates PtdIns-4,5-P2 synthesis: importance for calcium signaling and PI3K activity. Immunity *19*, 669–678.

Schamel, W.W.A., and Reth, M. (2000). Monomeric and oligomeric complexes of the B cell antigen receptor. Immunity *13*, 5–14.

Smith, F.D., and Scott, J.D. (2002). Signaling complexes: junctions on the intracellular information super highway. Curr. Biol. *12*, R32–R40.

Weng, G., Bhalla, U.S., and Iyengar, R. (1999). Complexity in biological signaling systems. Science *284*, 92–98.

Winslow, M.M., Neilson, J.R., and Crabtree, G.R. (2003). Calcium signaling in lymphocytes. Curr. Opin. Immunol. *15*, 299–307.

Yadava, N., Chandok, M.R., Prasad, J., Bhattacharya, S., Sopory, S.K., and Bhattacharya, A. (1997). Characterization of EhCaBP, a calcium-binding protein of *Entamoeba histolytica* and its binding proteins. Mol. Biochem. Parasitol. *84*, 69–82.

Yoshida, K., and Kufe, D. (2001). Negative regulation of the SHPTP1 protein tyrosine phosphates by protein kinase C in response to DNA damage. Mol. Pharmacol. *60*, 1431–1438.

Zhang, Z.Y. (1998). Protein tyrosine phosphatases: biological functions, structural characteristics and mechanisms of catalysis. Crit. Rev. Biochem. Mol. Biol. *33*, 1–52.